

# 000 001 002 003 004 005 006 007 008 009 010 011 012 013 014 015 016 017 018 019 020 021 022 023 024 025 026 027 028 029 030 031 032 033 034 035 036 037 038 039 040 041 042 043 044 045 046 047 048 049 050 051 052 053 AUTOENCODING-FREE CONTEXT COMPRESSION FOR LLMs VIA CONTEXTUAL SEMANTIC ANCHORS

**Anonymous authors**

Paper under double-blind review

## ABSTRACT

Context compression presents a promising approach for accelerating large language model (LLM) inference by compressing long contexts into compact representations. Current context compression methods predominantly rely on autoencoding tasks to train context-agnostic compression tokens to compress contextual semantics. While autoencoding tasks enable compression tokens to acquire compression capabilities, compression via autoencoding tasks creates a fundamental mismatch: the models are optimized for reconstruction that diverge from actual downstream tasks, thereby weakening the features more beneficial for real-world usage. We propose Semantic-Anchor Compression (SAC), a novel method that shifts from autoencoding task based compression to an architecture that is equipped with this compression capability *a priori*. Instead of training models to compress contexts through autoencoding tasks, SAC directly selects so-called anchor tokens from the original context and aggregates contextual information into their key-value (KV) representations. By deriving representations directly from the contextual tokens, SAC eliminates the need for autoencoding training. To ensure compression performance while directly leveraging anchor tokens, SAC incorporates two key designs: (1) anchor embeddings that enable the compressor to identify critical tokens, and (2) bidirectional attention modification that allows anchor tokens to capture information from the entire context. Experimental results demonstrate that SAC consistently outperforms existing context compression methods across various compression ratios. On out-of-distribution evaluation using MRQA, SAC achieves 1 EM improvement at 5x compression over strong baselines, with increasing advantages at higher compression ratios.

## 1 INTRODUCTION

The expanding scope of large language models (LLMs) to tasks like processing long documents (Liu et al., 2024b; Li et al., 2024; Duan et al., 2025), maintaining multi-turn dialogue coherence (Zhang et al., 2025; Yi et al., 2025; Guan et al., 2025), and generating responses grounded in extensive external knowledge (Lewis et al., 2020; Karpukhin et al., 2020; Huang et al., 2025) necessitates the incorporation of vast contexts into the model input. However, directly processing such extremely long contexts is fraught with challenges, including prohibitive computational costs, significant inference latency, and performance degradation, largely caused by the “lost-in-the-middle” phenomenon (Liu et al., 2024a).

To address these challenges, recent studies have proposed context compression (Chang et al., 2024; Li et al., 2025a), a technique that typically appends special tokens (i.e. compression tokens) to the end of the context and leverages the LLM’s causal attention mechanism to compress contextual information into a compact representation within these tokens. Once this compact representation is obtained, the LLM can generate responses conditioned on it, rather than being conditioned on the entire original context. This significant reduction in context length leads to substantial decreases in both inference time and GPU memory consumption. While effective, these approaches face a key limitation: the compression tokens are randomly initialized and lack inherent semantic information. To compensate, they typically rely on extensive pretraining on both autoencoding (AE) and language modeling (LM) tasks (illustrated in Figure 1) to endow the compression tokens with the ability to carry contextual information. While AE task has shown to be necessary in ICAE (Ge et al., 2024) since compression tokens lack context-relevant semantics, the AE task requires the compressed

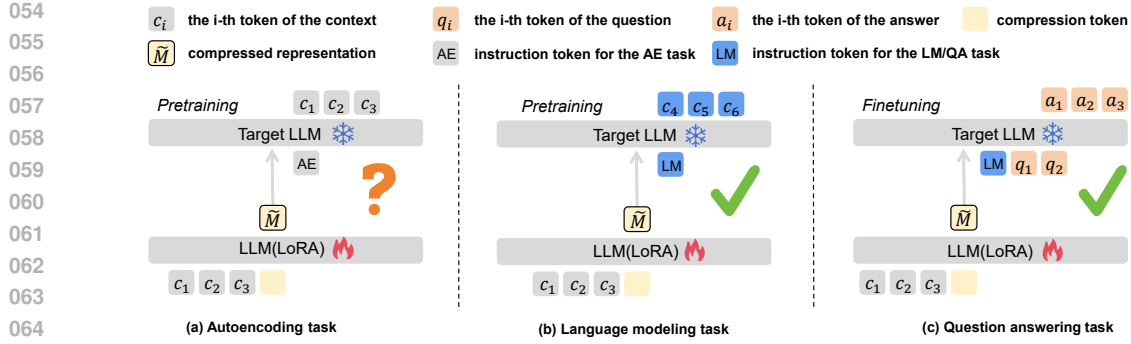


Figure 1: Three tasks for training the context compressor introduced by ICAE and followed by numerous works. The training uses (a) Autoencoding task and (b) Language modeling task to pretrain the encoder, then finetunes on (c) Question answering task.

representation to reconstruct all tokens in the context, even low-information tokens. This reliance on a suboptimal and costly pretraining stage raises a critical research question: Is it possible to design a compression architecture that inherently understands context without a demanding AE phase?

To answer this question, this work introduces Semantic-Anchor Compression (SAC) (Figure 2), a novel architecture for the context compression task. Instead of appending new special tokens and requiring extensive autoencoding pretraining to learn their representations, SAC directly selects representative tokens from the original context to act as ‘anchor tokens’ for compression. By leveraging these semantically meaningful anchors from the input itself, SAC incorporates natural semantic priors that obviate the need for autoencoding pretraining. To signify their special role, these selected tokens are then augmented with dedicated ‘anchor embeddings’, enabling the LLM to distinguish them from regular tokens. Furthermore, to enhance their compression capabilities, we modify the standard causal attention to a bidirectional attention mechanism. This allows anchor tokens to access information from the entire context, rather than being restricted to only preceding tokens. These modifications collectively foster a more effective context compression by providing anchor tokens with both distinct representations and comprehensive contextual awareness. Empirically, we test SAC on the MRQA (Fisch et al., 2019a) dataset and confirm that it outperforms existing strong context compression baselines. For example, compared to 500xCompressor (Li et al., 2025b) at 5x compression, the average exact match (EM) improves from 25.4 to 32.3. Results show that 1) our proposed method improves more in absolute accuracy over strong baselines on more challenging high compress ratio scenarios 2) our proposed architecture achieves its best performance in a simpler training setting without autoencoding training arguably because the anchor tokens already contain enough information about the original context. Our analysis reveals that SAC’s compressed representations more closely resemble original context token KVs in feature space, so that LLMs performing inference can arguably better understand them.

## 2 RELATED WORKS

### 2.1 COMPRESSION METHOD

Many methods focus on reducing prompt lengths. CC (Wingate et al., 2022) utilizes contrastive learning to compress specific natural language prompts into shorter and unique soft prompt tokens. However, it cannot generalize to unseen prompts and requires retraining for new prompts. GIST (Mu et al., 2023) compresses original prompts into KV values through finetuning and can handle arbitrary unseen contexts. AutoCompressor (Chevalier et al., 2023) recursively combines compressed vectors with sub-prompts and aggregates all compressed vectors to construct the final representation, enabling compression of longer contexts. However, both GIST and AutoCompressor require finetuning the LLMs performing inference (referred to later as target LLM), which may affect LLMs’ original capabilities.

ICAE (Ge et al., 2024) formulates context compression as training a general encoder that compresses contexts into compact representations understandable by target LLMs without finetuning. To achieve

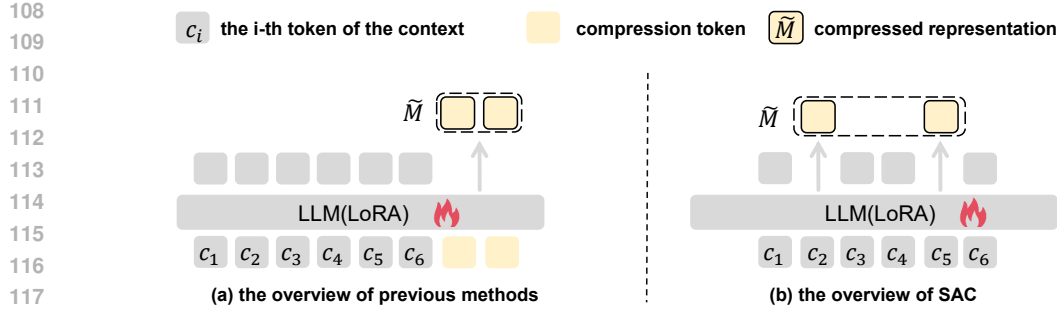


Figure 2: The difference between SAC and previous methods. While previous methods (a) compress contextual information into context-agnostic special tokens (referred to as compression tokens), SAC (b) compresses the context directly into the original contextual tokens themselves. Here,  $\tilde{M}$  can represent either the output from the final layer of the LLM or the Key-Value pairs, being later on used as compressed representations for LLM inference.

this, ICAE introduces autoencoding tasks and performs joint pretraining with language modeling tasks, followed by finetuning on downstream tasks. 500xCompressor (Li et al., 2025b) improves upon ICAE by replacing the compression carrier from the last layer output of compression tokens with KV values at each layer, achieving higher compression ratios. EPL (Zhao et al., 2025) identifies that ICAE and 500xCompressor neglect the impact of positional encoding and proposes distributing compression token position IDs uniformly across the entire context rather than placing them at the end. However, these methods still rely on autoencoding tasks to endow the compression tokens with the ability to carry contextual information.

Another category of prompt compression methods is based on token selection, which selects representative tokens from contexts based on token importance. SelectiveContext (Li et al., 2023), LLMLingua (Jiang et al., 2023), and LongLLMLingua (Jiang et al., 2024) employ causal small language models to evaluate token importance based on information entropy. LLMLingua-2 (Pan et al., 2024a) distills a token classifier to compute the probability of each token to be preserved. These works demonstrate that LLMs can understand original contexts using a small number of representative tokens. However, they do not perform compressed tokens training which limits the usability of the selected tokens by target LLMs. Our proposed SAC can be seen as a combination of token selection methods and compressed token training methods: it derives and train compressed representations that are based on tokens selected directly from the context and indeed is compatible with the token selection methods above.

## 2.2 BIDIRECTIONAL ATTENTION

Recent studies have shown that, removing the decoder’s unidirectional causal constraint and introducing bidirectional attention can effectively enhance the model’s representational capacity (Wang et al., 2020). For instance, NV-Embed (Lee et al., 2025) replaces causal attention with bidirectional attention during contrastive training, achieving strong performance on general text embedding and dense vector retrieval tasks. LLM2Vec (BehnamGhader et al., 2024), by enabling bidirectional attention alongside masked next-token prediction, significantly improves the model’s ability to capture global semantics in text embedding tasks. These works indicate that bidirectional attention is advantageous for acquiring global semantic information and robust contextual representations. However, its effectiveness in text compression tasks remains underexplored. Motivated by these findings, we incorporate bidirectional attention into the compressor to enhance contextual modeling during the compression phase.

162 3 METHOD  
163164 3.1 TASK FORMULATION  
165

166 Context compression is formally defined as follows: an encoder  $\mathcal{E}$  compresses a context  $C =$   
167  $(c_1, c_2, \dots, c_{|C|})$  into a compact representation  $\tilde{M}$  with  $\tilde{M} = \mathcal{E}(C)$ . Subsequently, a target LLM  
168 leverages the compressed representation  $\tilde{M}$  in place of the original context  $C$  to perform various  
169 tasks, such as question answering.

170 To train the encoder  $\mathcal{E}$  to effectively extract contextual information, ICAE introduces three objective  
171 functions. The autoencoding loss  $\mathcal{L}_{\text{AE}}$  ensures that the compressed representation  $\tilde{M}$  generated  
172 by  $\mathcal{E}$  preserves all tokens in the context  $C$ , regardless of their relative importance, as shown in  
173 Figure 1a; mathematically,  $\mathcal{L}_{\text{AE}} = -\log P(C|\tilde{M})$ . The language modeling loss  $\mathcal{L}_{\text{LM}}$  encourages  
174  $\tilde{M}$  to maintain predictive capability for future context  $C' = (c_{|C|+1}, c_{|C|+2}, \dots, c_{|C|+|C'|})$ , enabling  
175 proactive information planning, as shown in Figure 1b; mathematically,  $\mathcal{L}_{\text{LM}} = -\log P(C'|\tilde{M})$ .  
176 During pretraining,  $\mathcal{L}_{\text{AE}}$  and  $\mathcal{L}_{\text{LM}}$  are jointly optimized to obtain an initially effective encoder  $\mathcal{E}$ .  
177

178 Additionally, during finetuning, the question answering loss  $\mathcal{L}_{\text{QA}}$  enhances the ability of  $\tilde{M}$  to extract  
179 information that is potentially relevant for downstream tasks (e.g. QA). Since the encoder operates  
180 without knowledge of what questions might be asked later, it learns to identify and preserve information  
181 that is likely to be queried, enabling accurate answer generation  $A = (a_1, a_2, \dots, a_{|A|})$  when  
182 presented with subsequent questions  $Q = (q_1, q_2, \dots, q_{|Q|})$ , as shown in Figure 1c; mathematically,  
183  $\mathcal{L}_{\text{QA}} = -\log P(A|\tilde{M}, Q)$ .  
184

185 3.2 SEMANTIC-ANCHOR COMPRESSOR  
186

187 A key distinction between our approach SAC and previous methods is that we derive compressed  
188 representations directly from selected context tokens, as shown in Figure 2. This involves selecting a  
189 subset of tokens from context  $C$  as anchor tokens  $S \subseteq C$ . We believe that a good selection strategy  
190 benefits SAC. Following EPL, our default strategy divides the entire context  $C$  into  $|S|$  chunks and  
191 selects the middle token from each chunk. This setting helps maximize coverage of context  $C$ . As  
192 illustrated in Figure 3a, selected tokens  $c_i \in S$  are enhanced with anchor embeddings  $e_A$ , yielding an  
193 embedding sequence  $E = (e_1, e_2, \dots, e_{|C|})$ :  
194

$$e_i = \text{Emb}(c_i) + \mathbf{1}_{c_i \in S} \cdot e_A \quad (1)$$

195 where  $\mathbf{1}_{c_i \in S}$  is an indicator function that equals 1 when  $c_i \in S$  and 0 otherwise. Following  
196 previous works, we employ a LLM with LoRA parameters  $\theta_{\text{LoRA}}$  as the compressor:  $\tilde{M} = \mathcal{E}(C) =$   
197  $\text{LLM}(E|\theta_{\text{LoRA}})$ .

198 While using original tokens from the context avoids learning compressed tokens from scratch and  
199 potentially improves the learning efficiency. We notice that because the encoder uses causal attentions,  
200 the anchor tokens  $S$  do not have visibility to the full sentence, limiting its representation power.  
201 Hence we modify the LLM from using causal attention to use bidirectional attention (see Figure 3b),  
202 enhancing the LLM’s encoding capability.  $\tilde{M}$  can be either the output of anchor tokens from the  
203 LLM’s final layer or the Key-Value pairs from each layer. Following 500xCompressor, we use  
204 Key-Value pairs as the compressed representation  $\tilde{M}$ . During pretraining, we only use  $\mathcal{L}_{\text{LM}}$  and do  
205 not use  $\mathcal{L}_{\text{AE}}$  to train the compressor. Following previous work, we use  $\mathcal{L}_{\text{QA}}$  for finetuning.  
206

207 4 EXPERIMENTS  
208209 4.1 EXPERIMENTAL SETTING  
210

211 **Dataset.** For continued pretraining, we utilize the large-scale corpus SlimPajama-6B (Soboleva  
212 et al., 2023). During finetuning and evaluation, we employ the standard MRQA (Fisch et al., 2019b)  
213 question-answering dataset, which consolidates multiple QA tasks and standardizes them into a  
214 unified format. We evaluate SAC on both test sets, namely in-domain (ID) and out-of-domain  
215 (OOD), to comprehensively assess its in-distribution fitting ability and cross-domain generalization  
performance.

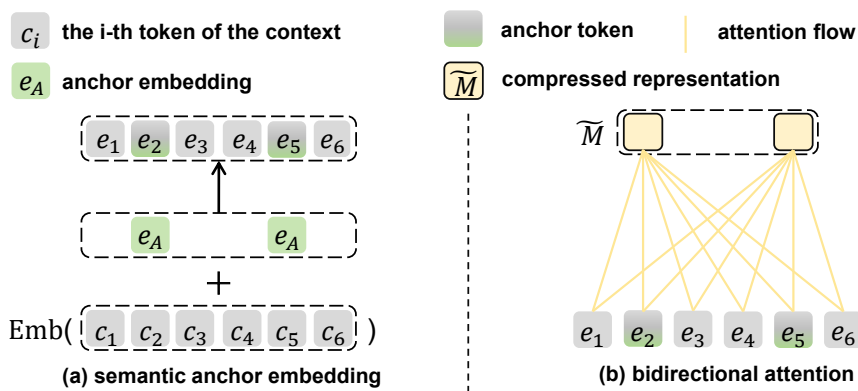


Figure 3: Key differentiators within SAC model architecture. (a) Representative tokens are transformed into anchor tokens through anchor embeddings. (b) The encoder in SAC adopts bidirectional attention, while the decoder operates with causal attention.

**Implementation Details.** SAC utilizes Llama-3.2-1B (Grattafiori & Dubey, 2024) as both the encoder and target LLM. The encoder is equipped with trainable LoRA (Hu et al., 2022) adapters (rank = 128,  $\alpha = 256$ ), while the target LLM parameters remain frozen. For each context, we partition it into sub-contexts of 510 tokens each. The compressor compresses each sub-context into a sub-compressed representation, and subsequently concatenates these sub-compressed representations to form the complete compressed representation. The number of anchor tokens  $|S| = \lfloor L/r \rfloor$  is determined by the compression ratio  $r$  and the length of the sub-context  $L$ . We train all models in two stages: pretraining for 20,000 optimization steps followed by finetuning for an additional 20,000 steps, both conducted with a batch size of 16. Complete hyperparameter configurations are provided in Appendix A.

**Baselines.** We use the Llama-3.2-1B model trained on the MRQA (Fisch et al., 2019b) dataset as an uncompressed baseline (denoted as "Full-FT"). We compare our method against several context compression techniques. For hard compression, we choose LLMLingua-2 (Pan et al., 2024b) and evaluate its performance on the Full-FT model. For soft compression, we select ICAE (Ge et al., 2024), 500xCompressor (Li et al., 2025b), and EPL (Zhao et al., 2025). To ensure a fair comparison, all these soft compression baselines are trained on the same dataset as our SAC method.

## 4.2 FINETUNING RESULTS

Tables 1 and 2 report the evaluation results of SAC on in-domain and out-of-domain MRQA datasets, which we analyze from three perspectives: overall performance, effect of compression ratio, and domain generalization.

**Overall Performance.** SAC consistently outperforms all baselines across a variety of conditions, including compression ratios, and both in-domain and out-of-domain tests, as shown in Tables 1 and 2. Averaging the results of the context compression methods across different compression ratios, SAC shows a maximum improvement of 24.6% F1 / 28.6% EM and a minimum improvement of 4.6% F1 / 5.7% EM in in-domain evaluations. For out-of-domain tests, the maximum improvement is 32.5% F1 / 36.2% EM, with a minimum improvement of 4.6% F1 / 6.9% EM.

**Impact of Compression Ratio.** We conducted a detailed evaluation of model performance under different compression ratios (5x, 15x, and 51x), as shown in Tables 1 and 2. As expected, F1 and EM scores of all methods decrease with increasing compression ratio, from 5x to 51x, since higher compression ratios result in more information being discarded. At the highest compression rate of 51x, the performance of different compression methods is not consistent. While one method may perform well on certain datasets, it may underperform on others. Nonetheless, SAC consistently achieves the best average performance.

**Cross-Domain Generalization.** We evaluated the generalization capability of SAC on out-of-domain datasets, as shown in Table 2. Under all compression ratio constraints, SAC consistently achieves the highest average F1/EM scores among all methods. Specifically, at a 5x compression ratio, SAC

270 Table 1: For the finetuning results, we report in-domain performance using ROUGE-1 F1 (Lin, 2004)  
 271 and exact match (EM) (Maalouly, 2022) scores on the following datasets: SQuAD (Rajpurkar et al.,  
 272 2016), NewsQA (Trischler et al., 2017), TriviaQA (Joshi et al., 2017), SearchQA (Dunn et al., 2017),  
 273 HotpotQA (Yang et al., 2018), and NaturalQuestions (NQ) (Kwiatkowski et al., 2019).

Methods	SQuAD		NewsQA		TriviaQA		SearchQA		HotpotQA		NQ		Avg	
	F1	EM												
Full-FT	77.69	59.71	63.5	46.04	68.80	60.54	73.25	62.07	74.78	59.26	71.01	53.47	71.51	56.85
Lingua-2	32.93	19.57	26.78	13.20	9.67	8.12	45.4	31.80	36.1	22.05	40.08	22.01	31.83	19.46
<i>5x compression constraint</i>														
ICAE	36.20	22.12	28.06	13.77	54.63	45.59	65.12	53.06	48.79	33.40	52.36	34.99	47.53	33.82
500x	51.62	33.63	39.70	22.63	57.62	48.76	66.43	54.38	59.10	42.20	57.11	39.26	55.26	40.14
EPL	64.72	44.28	48.74	<b>27.45</b>	63.75	54.54	69.69	57.73	67.16	49.79	63.32	44.16	62.90	46.33
SAC	<b>65.37</b>	<b>44.83</b>	<b>49.39</b>	27.14	<b>65.06</b>	<b>55.93</b>	<b>69.99</b>	<b>58.06</b>	<b>67.41</b>	<b>50.28</b>	<b>64.56</b>	<b>45.44</b>	<b>63.63</b>	<b>46.95</b>
<i>15x compression constraint</i>														
ICAE	31.90	18.91	25.25	11.97	51.78	42.94	64.81	52.89	45.22	30.32	48.01	30.67	44.50	31.28
500x	40.68	24.97	32.01	16.76	53.84	44.86	65.65	53.70	53.01	36.30	50.93	33.26	49.35	34.98
EPL	44.58	27.91	33.34	16.69	56.16	47.09	66.36	54.13	54.88	38.38	53.80	35.71	51.52	36.65
SAC	<b>47.43</b>	<b>30.25</b>	<b>36.55</b>	<b>18.07</b>	<b>61.13</b>	<b>52.19</b>	<b>68.97</b>	<b>56.76</b>	<b>58.83</b>	<b>41.86</b>	<b>56.79</b>	<b>38.88</b>	<b>54.95</b>	<b>39.67</b>
<i>51x compression constraint</i>														
ICAE	26.17	14.58	22.48	9.69	47.62	39.23	64.31	52.80	38.91	24.78	42.87	26.86	40.39	27.99
500x	30.09	17.11	25.06	12.20	50.84	42.13	64.92	53.29	42.15	27.32	46.07	29.53	43.19	30.26
EPL	30.09	17.49	24.49	11.54	51.15	42.38	65.12	53.16	42.19	27.23	46.29	29.77	43.22	30.26
SAC	<b>31.81</b>	<b>18.78</b>	<b>27.36</b>	<b>13.56</b>	<b>56.73</b>	<b>47.85</b>	<b>65.82</b>	<b>53.76</b>	<b>48.28</b>	<b>32.84</b>	<b>48.22</b>	<b>31.70</b>	<b>46.37</b>	<b>33.08</b>

290  
 291 attains average F1 and EM scores of 47.72 and 32.30, outperforming the second-best EPL method  
 292 by 0.77 and 1.0 points, respectively. At a more challenging 15x compression ratio, SAC achieves  
 293 average F1 and EM scores of 39.26 and 26.02, surpassing EPL by 2.52 and 2.19 points, with an EM  
 294 improvement approaching 10%. Even at an extreme 51x compression ratio, SAC maintains average  
 295 F1 and EM scores of 32.24 and 21.44, still leading EPL by 2.02 and 1.96 points, respectively. These  
 296 results indicate that the compressed representations learned by SAC exhibit strong cross-domain  
 297 robustness.

298  
 299 Table 2: For the finetuning results, we report out-of-domain performance using ROUGE-1 F1 and  
 300 exact match (EM) scores on the following datasets: BioASQ (Tsatsaronis et al., 2015), DROP (Dua  
 301 et al., 2019), DuoRC (Saha et al., 2018), RACE (Lai et al., 2017), Relation Extraction (RE) (Levy  
 302 et al., 2017), and TextbookQA (TQA) (Kembhavi et al., 2017).

Methods	BioASQ		DROP		DuoRC		RACE		RE		TQA		Avg	
	F1	EM	F1	EM	F1	EM	F1	EM	F1	EM	F1	EM	F1	EM
Full-FT	49.37	36.77	44.67	34.46	48.82	35.51	35.57	9.64	83.34	72.46	53.32	32.4	52.51	36.87
Lingua-2	27.76	19.48	27.28	18.83	27.07	18.32	17.54	4.15	39.30	20.59	28.42	15.83	27.90	16.20
<i>5x compression constraint</i>														
ICAE	36.08	26.06	28.95	21.09	16.67	10.79	15.65	3.12	54.73	41.01	35.24	20.96	31.22	20.51
500x	40.30	28.99	35.40	25.55	29.43	19.32	21.57	4.90	65.43	50.88	38.62	22.75	38.46	25.40
EPL	<b>46.05</b>	<b>32.58</b>	39.94	28.94	39.10	<b>27.12</b>	<b>30.99</b>	6.08	76.07	62.31	49.54	30.74	46.95	31.30
SAC	44.66	31.45	<b>41.55</b>	<b>30.87</b>	<b>39.48</b>	26.92	30.53	<b>6.23</b>	<b>77.87</b>	<b>65.40</b>	<b>52.24</b>	<b>32.93</b>	<b>47.72</b>	<b>32.30</b>
<i>15x compression constraint</i>														
ICAE	35.51	24.47	30.39	21.96	13.78	9.06	15.21	3.71	55.24	40.33	34.75	21.56	30.81	20.18
500x	36.30	25.93	33.46	23.55	20.53	12.72	18.49	3.41	54.37	41.11	41.09	25.82	34.04	22.09
EPL	40.52	28.52	32.16	22.29	25.70	16.39	20.97	4.01	59.75	46.34	41.31	25.42	36.74	23.83
SAC	<b>41.31</b>	<b>28.66</b>	<b>36.72</b>	<b>27.48</b>	<b>28.94</b>	<b>18.99</b>	<b>23.35</b>	<b>4.90</b>	<b>61.04</b>	<b>47.90</b>	<b>44.21</b>	<b>28.21</b>	<b>39.26</b>	<b>26.02</b>
<i>51x compression constraint</i>														
ICAE	33.82	23.67	27.94	19.29	11.14	6.86	14.89	3.41	47.02	34.02	33.08	19.83	27.98	17.85
500x	32.17	23.07	<b>30.11</b>	<b>21.76</b>	13.42	8.53	15.18	2.67	<b>54.62</b>	<b>41.86</b>	37.10	22.62	30.43	20.09
EPL	32.52	22.21	29.64	20.89	13.16	8.13	<b>17.15</b>	3.12	53.72	40.37	35.15	22.16	30.22	19.48
SAC	<b>36.95</b>	<b>26.86</b>	29.52	20.89	<b>21.85</b>	<b>14.26</b>	15.87	<b>4.00</b>	48.19	36.43	<b>41.05</b>	<b>26.21</b>	<b>32.24</b>	<b>21.44</b>

### 315 4.3 ABLATION STUDY

316 To verify the effectiveness of each key component and strategy in the SAC architecture, we conduct  
 317 three groups of ablation studies, all performed under a 5x compression ratio.

324 **Component Ablation.** As shown in Table 3, our ablation study clearly demonstrates the critical  
 325 roles of the bidirectional attention and anchor embedding. Removing either component leads to  
 326 substantial performance degradation in both in-domain (ID) and out-of-domain (OOD) settings. The  
 327 bidirectional attention mechanism enables anchor tokens to more effectively integrate information  
 328 from the entire context, producing compressed representations that are more beneficial for downstream  
 329 tasks. Meanwhile, the anchor embedding provides explicit structural signals that guide the model to  
 330 accurately identify and process these key tokens, thereby ensuring the effectiveness of information  
 331 compression.

332 Table 3: Component ablation results. We report the average F1/EM performance of the model on  
 333 in-domain (ID) and out-of-domain (OOD) tasks after removing the bidirectional attention (w/o mask)  
 334 and the anchor embedding (w/o anchor). Full results on all tasks are provided in the Appendix B.2.  
 335

Methods	ID						OOD					
	TriviaQA		HotpotQA		Avg		BioASQ		TextbookQA		Avg	
	F1	EM										
SAC	<b>65.06</b>	<b>55.93</b>	<b>67.41</b>	<b>50.28</b>	<b>66.24</b>	<b>53.11</b>	<b>44.66</b>	31.45	<b>52.24</b>	<b>32.93</b>	<b>48.45</b>	<b>32.19</b>
SAC(w/o mask)	62.60	53.27	64.63	47.43	63.62	50.35	41.93	30.65	48.29	29.67	45.11	30.16
SAC(w/o anchor)	63.90	54.81	65.25	48.31	64.58	51.56	43.70	<b>31.78</b>	51.59	32.20	47.65	31.99

342 **Token Selection.** As shown in Table 4, our ablation study investigates the effect of different token  
 343 selection strategies on the performance of SAC. The results indicate that random selection (*Random*)  
 344 significantly degrades performance, not only because the selected tokens lack importance, but also  
 345 due to their positional randomness, which leads to insufficient global coverage and fails to effectively  
 346 represent the context. In contrast, both information-based selection (*Lingua-2*) and our default strategy  
 347 achieve near-optimal results, and both substantially outperform existing baselines in Tables 1 and 2.  
 348 This demonstrates that the SAC architecture can effectively leverage and enhance any high-quality  
 349 token selection strategy, rather than relying on a specific choice, highlighting the generality and  
 350 robustness of the SAC framework.

351 Table 4: Token selection ablation results. This table demonstrates how different token selection  
 352 strategies affect model performance, comparing Random selection, Lingua-2-based selection (Pan  
 353 et al., 2024b), and our uniform selection (Zhao et al., 2025). We report average F1/EM scores across  
 354 in-domain (ID) and out-of-domain (OOD) tasks, with comprehensive results for all individual tasks  
 355 presented in the Appendix B.2.

Methods	ID						OOD					
	TriviaQA		HotpotQA		Avg		BioASQ		TextbookQA		Avg	
	F1	EM										
SAC	<b>65.06</b>	<b>55.93</b>	<b>67.41</b>	<b>50.28</b>	<b>66.24</b>	<b>53.11</b>	<b>44.66</b>	31.45	<b>52.24</b>	<b>32.93</b>	<b>48.45</b>	<b>32.19</b>
SAC(Random)	59.24	50.22	58.84	41.86	59.04	46.04	43.18	30.59	45.36	29.27	44.27	29.93
SAC(Lingua-2)	64.55	55.13	67.05	49.74	65.80	52.44	44.49	<b>31.91</b>	51.46	32.07	47.98	31.99

362 **AE Effect.** As shown in Table 5, we compare the effect of introducing an autoencoding (AE) objective  
 363 during training on the performance of SAC. Traditional context compression methods employ AE  
 364 tasks to force independent compression tokens to attend to the original context for reconstruction.  
 365 However, we find that the AE objective itself has inherent limitations, as its reconstruction target is  
 366 misaligned with downstream tasks. The experimental results validate this observation: training with  
 367 only the AE objective leads to a substantial performance drop, and even when combined with the  
 368 LM objective, the performance still lags behind the full SAC model. This highlights the architectural  
 369 advantage of SAC: since anchor tokens are naturally semantically aligned with the original context,  
 370 our method does not require AE objectives to force learning. Instead, SAC effectively aggregates  
 371 contextual information into anchor token representations solely through anchor embeddings and  
 372 bidirectional attention. It is worth noting that the ablation experiments in ICAE demonstrate that  
 373 combining autoencoding tasks with language modeling tasks yields better results (Ge et al., 2024).  
 374 However, our reproduction on 500xCompressor does not fully support this finding. Specifically,  
 375 under 15x and 51x compression ratios, 500xCompressor achieves better in-distribution (ID) results  
 376 when using language modeling tasks alone, with other scenarios being exceptions. This observation  
 377 raises questions regarding the necessity of autoencoding tasks and suggests that autoencoding may  
 378 not be entirely essential for context compression methods.

378 Table 5: Ablation study on the effects of autoencoding (AE) and language modeling (LM) objectives.  
379

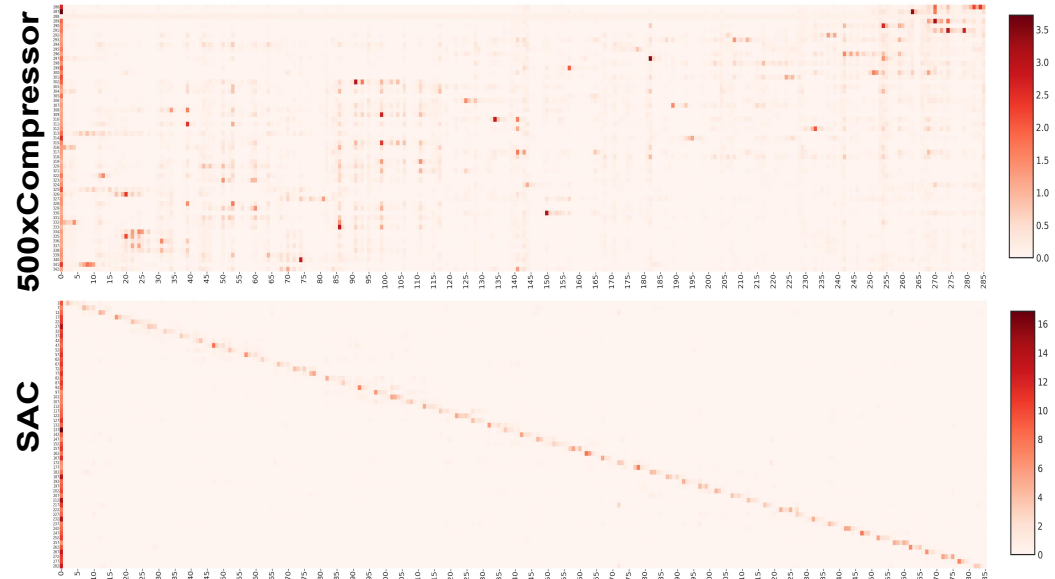
380 381 382 383 384 385 386 387 388 389 390 391 392 393 394 395 396 397 398 399 400 401 402 403 404 405 406 407 408 409 410 411 412 413 414 415 416 417 418 419 420 421 422 423 424 425 426 427 428 429 430 431	ID												OOD																								
	Methods	5x						15x						51x						5x						15x						51x					
		F1		EM		F1		EM		F1		EM		F1		EM		F1		EM		F1		EM		F1		EM									
SAC	<b>63.63</b>	<b>46.95</b>	<b>54.95</b>	<b>39.67</b>	<b>46.37</b>	<b>33.08</b>	<b>47.72</b>	<b>32.30</b>	<b>39.26</b>	<b>26.02</b>	<b>32.24</b>	<b>21.44</b>	53.23	38.70	49.76	35.71	44.46	31.41	38.22	25.73	33.99	22.05	30.09	18.99	55.26	40.14	49.35	34.98	43.19	30.26	38.46	25.40	34.04	22.09	30.43	20.09	
500x(w/ LM only)	500x(w/ AE+LM)	56.55	40.34	49.93	35.33	43.95	30.64	42.08	27.98	35.50	23.29	28.77	18.32	56.55	40.34	49.93	35.33	43.95	30.64	42.08	27.98	35.50	23.29	28.77	18.32	62.04	45.80	51.73	36.67	44.69	31.37	47.26	32.25	37.23	23.96	31.01	19.90
SAC(w/ AE only)	SAC(w/ AE+LM)																																				

## 388 5 ANALYSIS

### 389 5.1 ATTENTION VISUALIZATION

392 To understand the unique behavior of compressed models, we analyzed the attention patterns of the  
393 final layer at a 5x compression rate. Attention maps for other compression rates can be found in  
394 Appendix C.2.

395 As observed in Figure 4, The attention map for the 500xCompressor exhibits a distinct anti-diagonal  
396 trend. To complete the autoencoding task, the model must condense the entire original sequence into  
397 these remaining compressed tokens. This forces later compressed tokens to break locality constraints  
398 and actively seek out and attend to distant but important tokens in the sequence. In contrast, the  
399 SAC model demonstrates a clear diagonal pattern, where its anchor tokens effectively attend to their  
400 neighboring original context tokens, showing a better ability to focus on local information.



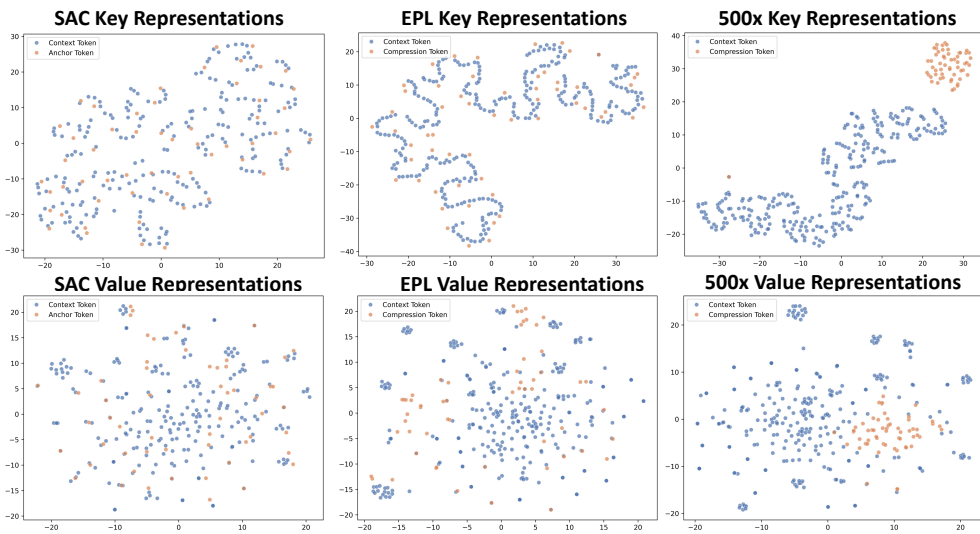
411 Figure 4: Attention maps of different models finetuned under a 5x compression rate. From top to bottom, the figure displays the final layer attention maps for the 500xCompressor and SAC  
412 models, respectively. The x-axis represents the original context tokens, and the y-axis represents the  
413 compression/anchor tokens.

### 427 5.2 REPRESENTATION ANALYSIS

428 **Key Representation Analysis.** In the Key representation space (see Figure 5), the compression  
429 tokens (orange) of SAC and EPL are distributed relatively close to the context tokens (blue), while  
430 the compression tokens of 500xCompressor are clearly separated from the context tokens. This  
431 discrepancy arises from the architectural design of each method. Specifically, although the positional

432 IDs of 500xCompressor’s additional compression tokens are contiguous, their semantics are not  
 433 aligned, leading to a complete separation in the Key space. In contrast, EPL modifies the positional  
 434 IDs of its additional compression tokens to share the same rotational angle (RoPE) as the original  
 435 context tokens, thereby reducing the distance between them. However, in SAC, the anchor tokens are  
 436 directly embedded within the original context, and their representations maintain close semantic ties  
 437 with the context tokens from the outset, naturally preventing significant representational divergence.

438 **Value Representation Analysis.** In the Value representation space (see Figure 5), the anchor tokens  
 439 of SAC are uniformly distributed across all regions with the Value representations of the context  
 440 tokens, without forming independent sub-clusters. This suggests that SAC’s anchor embedding  
 441 strategy allows for compressed Value representations that more closely match the distribution of  
 442 the original Value space. In contrast, although EPL’s compression tokens also overlap with the  
 443 context tokens, their distribution is less complete than SAC’s: they appear relatively sparse in the  
 444 core regions and show a slight clustering tendency at the boundaries. This indicates that EPL’s Value  
 445 representations still exhibit a degree of semantic shift relative to the original Value space, which is  
 446 even more pronounced in the 500xCompressor.



465 Figure 5: The t-SNE visualization shows the key representations of the final layer KV values for  
 466 SAC, 500xCompressor (Li et al., 2025b), and EPL (Zhao et al., 2025), respectively.

## 469 6 CONCLUSION

471 This paper proposes a novel, autoencoding-free context compression method, **Semantic-Anchor**  
 472 **Compression (SAC)**, designed to address the performance degradation in downstream tasks caused  
 473 by context-agnostic compression tokens and autoencoding objectives in existing context compression  
 474 methods. Unlike traditional context compression approaches, SAC does not rely on training compres-  
 475 sion tokens to reconstruct the original input. Instead, it directly selects representative *anchor* tokens  
 476 from the context and aggregates contextual information into their key-value (KV) representations  
 477 via a bidirectional attention mechanism. This approach effectively compresses lengthy contexts  
 478 while avoiding any impairment to the language model’s original language modeling capabilities.  
 479 Experiments on multiple question answering tasks demonstrate that SAC achieves a high compression  
 480 ratio and significantly outperforms existing compression methods, highlighting its superiority in  
 481 balancing compression efficiency and model performance.

## 482 7 REPRODUCIBILITY STATEMENT

483 We declare that the work presented in this paper is reproducible. We provide a link to our anonymous  
 484 source code as supplementary material: <https://anonymous.4open.science/r/SAC-E32C>. This code

486 can be used to reproduce the experimental results. The repository includes detailed instructions for  
 487 environment setup, running experiments, data processing, and result evaluation.  
 488

489 **REFERENCES**  
 490

491 Parishad BehnamGhader, Vaibhav Adlakha, Marius Mosbach, Dzmitry Bahdanau, Nicolas Chapados,  
 492 and Siva Reddy. Llm2vec: Large language models are secretly powerful text encoders, 2024. URL  
 493 <https://arxiv.org/abs/2404.05961>.

494 Kaiyan Chang, Songcheng Xu, Chenglong Wang, Yingfeng Luo, Xiaoqian Liu, Tong Xiao, and  
 495 Jingbo Zhu. Efficient prompting methods for large language models: A survey, 2024. URL  
 496 <https://arxiv.org/abs/2404.01077>.

497 Alexis Chevalier, Alexander Wettig, Anirudh Ajith, and Danqi Chen. Adapting language models to  
 498 compress contexts. In Houda Bouamor, Juan Pino, and Kalika Bali (eds.), *Proceedings of the 2023*  
 499 *Conference on Empirical Methods in Natural Language Processing*, pp. 3829–3846, Singapore,  
 500 December 2023. Association for Computational Linguistics. doi: 10.18653/v1/2023.emnlp-main.  
 501 232. URL <https://aclanthology.org/2023.emnlp-main.232>.

502 Dheeru Dua, Yizhong Wang, Pradeep Dasigi, Gabriel Stanovsky, Sameer Singh, and Matt Gardner.  
 503 DROP: A reading comprehension benchmark requiring discrete reasoning over paragraphs. In  
 504 Jill Burstein, Christy Doran, and Thamar Solorio (eds.), *Proceedings of the 2019 Conference of*  
 505 *the North American Chapter of the Association for Computational Linguistics: Human Language*  
 506 *Technologies, Volume 1 (Long and Short Papers)*, pp. 2368–2378, Minneapolis, Minnesota, June  
 507 2019. Association for Computational Linguistics. doi: 10.18653/v1/N19-1246. URL <https://aclanthology.org/N19-1246>.

508 Shaohua Duan, Xinze Li, Zhenghao Liu, Xiaoyuan Yi, Yukun Yan, Shuo Wang, Yu Gu, Ge Yu,  
 509 and Maosong Sun. Chunks as arms: Multi-armed bandit-guided sampling for long-context llm  
 510 preference optimization. *arXiv preprint arXiv:2508.13993*, 2025.

511 Matthew Dunn, Levent Sagun, Mike Higgins, V. Ugur Güney, Volkan Cirik, and Kyunghyun Cho.  
 512 Searchqa: A new q&a dataset augmented with context from a search engine. *CoRR*, abs/1704.05179,  
 513 2017. URL <http://arxiv.org/abs/1704.05179>.

514 Adam Fisch, Alon Talmor, Robin Jia, Minjoon Seo, Eunsol Choi, and Danqi Chen. MRQA 2019  
 515 shared task: Evaluating generalization in reading comprehension. In Adam Fisch, Alon Talmor,  
 516 Robin Jia, Minjoon Seo, Eunsol Choi, and Danqi Chen (eds.), *Proceedings of the 2nd Workshop*  
 517 *on Machine Reading for Question Answering*, pp. 1–13, Hong Kong, China, November 2019a.  
 518 Association for Computational Linguistics. doi: 10.18653/v1/D19-5801. URL <https://aclanthology.org/D19-5801>.

519 Adam Fisch, Alon Talmor, Robin Jia, Minjoon Seo, Eunsol Choi, and Danqi Chen. MRQA 2019  
 520 shared task: Evaluating generalization in reading comprehension. In *Proceedings of 2nd Machine*  
 521 *Reading for Reading Comprehension (MRQA) Workshop at EMNLP*, 2019b.

522 Tao Ge, Jing Hu, Lei Wang, Xun Wang, Si-Qing Chen, and Furu Wei. In-context autoencoder  
 523 for context compression in a large language model, 2024. URL <https://arxiv.org/abs/2307.06945>.

524 Aaron Grattafiori and Abhimanyu Dubey. The llama 3 herd of models, 2024. URL <https://arxiv.org/abs/2407.21783>.

525 Shengyue Guan, Haoyi Xiong, Jindong Wang, Jiang Bian, Bin Zhu, and Jian guang Lou. Evaluating  
 526 llm-based agents for multi-turn conversations: A survey, 2025. URL <https://arxiv.org/abs/2503.22458>.

527 Edward J Hu, Yelong Shen, Phillip Wallis, Zeyuan Allen-Zhu, Yuanzhi Li, Shean Wang, Lu Wang,  
 528 and Weizhu Chen. LoRA: Low-rank adaptation of large language models. In *International*  
 529 *Conference on Learning Representations*, 2022. URL <https://openreview.net/forum?id=nZeVKeFYf9>.

540 Pengcheng Huang, Zhenghao Liu, Yukun Yan, Xiaoyuan Yi, Hao Chen, Zhiyuan Liu, Maosong Sun,  
 541 Tong Xiao, Ge Yu, and Chenyan Xiong. Pip-kag: Mitigating knowledge conflicts in knowledge-  
 542 augmented generation via parametric pruning. *arXiv preprint arXiv:2502.15543*, 2025.

543

544 Huiqiang Jiang, Qianhui Wu, Chin-Yew Lin, Yuqing Yang, and Lili Qiu. LLMLingua: Com-  
 545 pressing prompts for accelerated inference of large language models. In Houda Bouamor,  
 546 Juan Pino, and Kalika Bali (eds.), *Proceedings of the 2023 Conference on Empirical Meth-  
 547 ods in Natural Language Processing*, pp. 13358–13376, Singapore, December 2023. Associa-  
 548 tion for Computational Linguistics. doi: 10.18653/v1/2023.emnlp-main.825. URL <https://aclanthology.org/2023.emnlp-main.825/>.

549

550 Huiqiang Jiang, Qianhui Wu, Xufang Luo, Dongsheng Li, Chin-Yew Lin, Yuqing Yang, and Lili  
 551 Qiu. LongLLMLingua: Accelerating and enhancing LLMs in long context scenarios via prompt  
 552 compression. In Lun-Wei Ku, Andre Martins, and Vivek Srikumar (eds.), *Proceedings of the 62nd  
 553 Annual Meeting of the Association for Computational Linguistics (Volume 1: Long Papers)*, pp.  
 554 1658–1677, Bangkok, Thailand, August 2024. Association for Computational Linguistics. doi: 10.  
 555 18653/v1/2024.acl-long.91. URL <https://aclanthology.org/2024.acl-long.91/>.

556

557 Mandar Joshi, Eunsol Choi, Daniel Weld, and Luke Zettlemoyer. TriviaQA: A large scale  
 558 distantly supervised challenge dataset for reading comprehension. In Regina Barzilay and  
 559 Min-Yen Kan (eds.), *Proceedings of the 55th Annual Meeting of the Association for Com-  
 560 putational Linguistics (Volume 1: Long Papers)*, pp. 1601–1611, Vancouver, Canada, July  
 561 2017. Association for Computational Linguistics. doi: 10.18653/v1/P17-1147. URL <https://aclanthology.org/P17-1147/>.

562

563 Vladimir Karpukhin, Barlas Onguz, Sewon Min, Patrick Lewis, Ledell Wu, Sergey Edunov, Danqi  
 564 Chen, and Wen-tau Yih. Dense passage retrieval for open-domain question answering. In Bonnie  
 565 Webber, Trevor Cohn, Yulan He, and Yang Liu (eds.), *Proceedings of the 2020 Conference on  
 566 Empirical Methods in Natural Language Processing (EMNLP)*, pp. 6769–6781, Online, November  
 567 2020. Association for Computational Linguistics. doi: 10.18653/v1/2020.emnlp-main.550. URL  
<https://aclanthology.org/2020.emnlp-main.550/>.

568

569 Aniruddha Kembhavi, Minjoon Seo, Dustin Schwenk, Jonghyun Choi, Ali Farhadi, and Hannaneh  
 570 Hajishirzi. Are you smarter than a sixth grader? textbook question answering for multimodal  
 571 machine comprehension. In *Proceedings of the IEEE Conference on Computer Vision and Pattern  
 572 Recognition (CVPR)*, July 2017.

573

574 Tom Kwiatkowski, Jennimaria Palomaki, Olivia Redfield, Michael Collins, Ankur Parikh, Chris  
 575 Alberti, Danielle Epstein, Illia Polosukhin, Matthew Kelcey, Jacob Devlin, Kenton Lee, Kristina N.  
 576 Toutanova, Llion Jones, Ming-Wei Chang, Andrew Dai, Jakob Uszkoreit, Quoc Le, and Slav Petrov.  
 577 Natural questions: a benchmark for question answering research. *Transactions of the Association  
 578 of Computational Linguistics*, 2019.

579

580 Guokun Lai, Qizhe Xie, Hanxiao Liu, Yiming Yang, and Eduard Hovy. RACE: Large-scale ReAding  
 581 comprehension dataset from examinations. In Martha Palmer, Rebecca Hwa, and Sebastian Riedel  
 582 (eds.), *Proceedings of the 2017 Conference on Empirical Methods in Natural Language Processing*,  
 583 pp. 785–794, Copenhagen, Denmark, September 2017. Association for Computational Linguistics.  
 584 doi: 10.18653/v1/D17-1082. URL <https://aclanthology.org/D17-1082/>.

585

586 Chankyu Lee, Rajarshi Roy, Mengyao Xu, Jonathan Raiman, Mohammad Shoeybi, Bryan Catanzaro,  
 587 and Wei Ping. Nv-embed: Improved techniques for training llms as generalist embedding models,  
 588 2025. URL <https://arxiv.org/abs/2405.17428>.

589

590 Omer Levy, Minjoon Seo, Eunsol Choi, and Luke Zettlemoyer. Zero-shot relation extraction via  
 591 reading comprehension. In Roger Levy and Lucia Specia (eds.), *Proceedings of the 21st Conference  
 592 on Computational Natural Language Learning (CoNLL 2017)*, pp. 333–342, Vancouver, Canada,  
 593 August 2017. Association for Computational Linguistics. doi: 10.18653/v1/K17-1034. URL  
<https://aclanthology.org/K17-1034/>.

594

595 Patrick Lewis, Ethan Perez, Aleksandra Piktus, Fabio Petroni, Vladimir Karpukhin, Naman Goyal,  
 596 Heinrich Küttler, Mike Lewis, Wen-tau Yih, Tim Rockäschel, Sebastian Riedel, and Douwe Kiela.  
 597 Retrieval-augmented generation for knowledge-intensive nlp tasks. In *Proceedings of the 34th*

594      *International Conference on Neural Information Processing Systems, NIPS '20*, Red Hook, NY,  
 595      USA, 2020. Curran Associates Inc. ISBN 9781713829546.

596

597      Jiaqi Li, Mengmeng Wang, Zilong Zheng, and Muhan Zhang. LooGLE: Can long-context  
 598      language models understand long contexts? In Lun-Wei Ku, Andre Martins, and Vivek  
 599      Srikumar (eds.), *Proceedings of the 62nd Annual Meeting of the Association for Compu-  
 600      tational Linguistics (Volume 1: Long Papers)*, pp. 16304–16333, Bangkok, Thailand, August  
 601      2024. Association for Computational Linguistics. doi: 10.18653/v1/2024.acl-long.859. URL  
 602      <https://aclanthology.org/2024.acl-long.859/>.

603

604      Yucheng Li, Bo Dong, Frank Guerin, and Chenghua Lin. Compressing context to enhance inference  
 605      efficiency of large language models. In Houda Bouamor, Juan Pino, and Kalika Bali (eds.), *Pro-  
 606      ceedings of the 2023 Conference on Empirical Methods in Natural Language Processing*, pp. 6342–  
 607      6353, Singapore, December 2023. Association for Computational Linguistics. doi: 10.18653/v1/  
 2023.emnlp-main.391. URL <https://aclanthology.org/2023.emnlp-main.391/>.

608      Zongqian Li, Yinhong Liu, Yixuan Su, and Nigel Collier. Prompt compression for large language  
 609      models: A survey. In Luis Chiruzzo, Alan Ritter, and Lu Wang (eds.), *Proceedings of the 2025  
 610      Conference of the Nations of the Americas Chapter of the Association for Computational Linguis-  
 611      tics: Human Language Technologies (Volume 1: Long Papers)*, pp. 7182–7195, Albuquerque,  
 612      New Mexico, April 2025a. Association for Computational Linguistics. ISBN 979-8-89176-  
 613      189-6. doi: 10.18653/v1/2025.naacl-long.368. URL <https://aclanthology.org/2025.naacl-long.368/>.

614

615      Zongqian Li, Yixuan Su, and Nigel Collier. 500xCompressor: Generalized prompt compression  
 616      for large language models. In Wanxiang Che, Joyce Nabende, Ekaterina Shutova, and Mo-  
 617      hammad Taher Pilehvar (eds.), *Proceedings of the 63rd Annual Meeting of the Association for  
 618      Computational Linguistics (Volume 1: Long Papers)*, pp. 25081–25091, Vienna, Austria, July  
 619      2025b. Association for Computational Linguistics. ISBN 979-8-89176-251-0. doi: 10.18653/v1/  
 620      2025.acl-long.1219. URL <https://aclanthology.org/2025.acl-long.1219/>.

621

622      Chin-Yew Lin. ROUGE: A package for automatic evaluation of summaries. In *Text Summarization  
 623      Branches Out*, pp. 74–81, Barcelona, Spain, July 2004. Association for Computational Linguistics.  
 624      URL <https://aclanthology.org/W04-1013/>.

625

626      Nelson F. Liu, Kevin Lin, John Hewitt, Ashwin Paranjape, Michele Bevilacqua, Fabio Petroni, and  
 627      Percy Liang. Lost in the middle: How language models use long contexts. *Transactions of the  
 628      Association for Computational Linguistics*, 12:157–173, 2024a. doi: 10.1162/tacl\_a\_00638. URL  
 629      <https://aclanthology.org/2024.tacl-1.9/>.

630

631      Xinyu Liu, Runsong Zhao, Pengcheng Huang, Chunyang Xiao, Bei Li, Jingang Wang, Tong Xiao,  
 632      and Jingbo Zhu. Forgetting curve: A reliable method for evaluating memorization capability for  
 633      long-context models. *arXiv preprint arXiv:2410.04727*, 2024b.

634

635      Nicolas El Maalouly. Exact matching: Algorithms and related problems, 2022. URL <https://arxiv.org/abs/2203.13899>.

636

637      Jesse Mu, Xiang Lisa Li, and Noah Goodman. Learning to compress prompts with gist tokens.  
 638      In *Thirty-seventh Conference on Neural Information Processing Systems*, 2023. URL <https://openreview.net/forum?id=2DtxPCL3T5>.

639

640      Zhuoshi Pan, Qianhui Wu, Huiqiang Jiang, Menglin Xia, Xufang Luo, Jue Zhang, Qingwei Lin, Victor  
 641      Rühle, Yuqing Yang, Chin-Yew Lin, H. Vicky Zhao, Lili Qiu, and Dongmei Zhang. LLMLingua-2:  
 642      Data distillation for efficient and faithful task-agnostic prompt compression. In Lun-Wei Ku, Andre  
 643      Martins, and Vivek Srikumar (eds.), *Findings of the Association for Computational Linguistics:  
 644      ACL 2024*, pp. 963–981, Bangkok, Thailand, August 2024a. Association for Computational  
 645      Linguistics. doi: 10.18653/v1/2024.findings-acl.57. URL <https://aclanthology.org/2024.findings-acl.57/>.

646

647      Zhuoshi Pan, Qianhui Wu, Huiqiang Jiang, Menglin Xia, Xufang Luo, Jue Zhang, Qingwei Lin, Victor  
 648      Rühle, Yuqing Yang, Chin-Yew Lin, H. Vicky Zhao, Lili Qiu, and Dongmei Zhang. LLMLingua-  
 649      2: Data distillation for efficient and faithful task-agnostic prompt compression, 2024b. URL  
 650      <https://arxiv.org/abs/2403.12968>.

648 Pranav Rajpurkar, Jian Zhang, Konstantin Lopyrev, and Percy Liang. SQuAD: 100,000+ questions  
 649 for machine comprehension of text. In Jian Su, Kevin Duh, and Xavier Carreras (eds.), *Proceedings*  
 650 *of the 2016 Conference on Empirical Methods in Natural Language Processing*, pp. 2383–2392,  
 651 Austin, Texas, November 2016. Association for Computational Linguistics. doi: 10.18653/v1/

652 D16-1264. URL <https://aclanthology.org/D16-1264/>.

653

654 Amrita Saha, Rahul Aralikatte, Mitesh M. Khapra, and Karthik Sankaranarayanan. DuoRC: Towards  
 655 complex language understanding with paraphrased reading comprehension. In Iryna Gurevych and  
 656 Yusuke Miyao (eds.), *Proceedings of the 56th Annual Meeting of the Association for Computational*  
 657 *Linguistics (Volume 1: Long Papers)*, pp. 1683–1693, Melbourne, Australia, July 2018. Association  
 658 for Computational Linguistics. doi: 10.18653/v1/P18-1156. URL <https://aclanthology.org/P18-1156/>.

659

660 Daria Soboleva, Faisal Al-Khateeb, Robert Myers, Jacob R Steeves, Joel Hestness, and  
 661 Nolan Dey. SlimPajama: A 627B token cleaned and deduplicated version of RedPa-  
 662 jama. <https://www.cerebras.net/blog/slimpajama>, 2023. URL <https://huggingface.co/datasets/cerebras/SlimPajama-627B>.

663

664 Adam Trischler, Tong Wang, Xingdi Yuan, Justin Harris, Alessandro Sordoni, Philip Bachman,  
 665 and Kaheer Suleman. NewsQA: A machine comprehension dataset. In Phil Blunsom, An-  
 666 toine Bordes, Kyunghyun Cho, Shay Cohen, Chris Dyer, Edward Grefenstette, Karl Moritz  
 667 Hermann, Laura Rimell, Jason Weston, and Scott Yih (eds.), *Proceedings of the 2nd Work-  
 668 shop on Representation Learning for NLP*, pp. 191–200, Vancouver, Canada, August 2017.  
 669 Association for Computational Linguistics. doi: 10.18653/v1/W17-2623. URL <https://aclanthology.org/W17-2623/>.

670

671

672 George Tsatsaronis, Georgios Balikas, Prodromos Malakasiotis, Ioannis Partalas, Matthias Zschunke,  
 673 Michael R. Alvers, Dirk Weissenborn, Anastasia Krithara, Sergios Petridis, Dimitris Poly-  
 674 chronopoulos, Yannis Almirantis, John Pavlopoulos, Nicolas Baskiotis, Patrick Gallinari, Thierry  
 675 Artières, Axel-Cyrille Ngonga Ngomo, Norman Heino, Eric Gaussier, Liliana Barrio-Alvers,  
 676 Michael Schroeder, Ion Androutsopoulos, and Georgios Palioras. An overview of the BIOASQ  
 677 large-scale biomedical semantic indexing and question answering competition. *BMC Bioin-  
 678 formatics*, 16(1):138, 2015. ISSN 1471-2105. doi: 10.1186/s12859-015-0564-6. URL  
 679 <https://doi.org/10.1186/s12859-015-0564-6>.

680

681 Alex Wang, Yada Pruksachatkun, Nikita Nangia, Amanpreet Singh, Julian Michael, Felix Hill, Omer  
 682 Levy, and Samuel R. Bowman. SuperGLUE: A stickier benchmark for general-purpose language  
 683 understanding systems, 2020. URL <https://arxiv.org/abs/1905.00537>.

684

685 David Wingate, Mohammad Shoeybi, and Taylor Sorensen. Prompt compression and contrastive  
 686 conditioning for controllability and toxicity reduction in language models. In Yoav Goldberg,  
 687 Zornitsa Kozareva, and Yue Zhang (eds.), *Findings of the Association for Computational Lin-  
 688 guistics: EMNLP 2022*, pp. 5621–5634, Abu Dhabi, United Arab Emirates, December 2022.  
 689 Association for Computational Linguistics. doi: 10.18653/v1/2022.findings-emnlp.412. URL  
 690 <https://aclanthology.org/2022.findings-emnlp.412/>.

691

692 Zhilin Yang, Peng Qi, Saizheng Zhang, Yoshua Bengio, William Cohen, Ruslan Salakhutdinov, and  
 693 Christopher D. Manning. HotpotQA: A dataset for diverse, explainable multi-hop question answer-  
 694 ing. In Ellen Riloff, David Chiang, Julia Hockenmaier, and Jun’ichi Tsujii (eds.), *Proceedings*  
 695 *of the 2018 Conference on Empirical Methods in Natural Language Processing*, pp. 2369–2380,  
 Brussels, Belgium, October–November 2018. Association for Computational Linguistics. doi:  
 10.18653/v1/D18-1259. URL <https://aclanthology.org/D18-1259/>.

696

697 Zihao Yi, Jiarui Ouyang, Zhe Xu, Yuwen Liu, Tianhao Liao, Haohao Luo, and Ying Shen. A survey  
 698 on recent advances in ILM-based multi-turn dialogue systems, 2025. URL <https://arxiv.org/abs/2402.18013>.

699

700 Chen Zhang, Xinyi Dai, Yaxiong Wu, Qu Yang, Yasheng Wang, Ruiming Tang, and Yong Liu.  
 701 A survey on multi-turn interaction capabilities of large language models, 2025. URL <https://arxiv.org/abs/2501.09959>.

702 Runsong Zhao, Xin Liu, Xinyu Liu, Pengcheng Huang, Chunyang Xiao, Tong Xiao, and Jingbo  
703 Zhu. Position ids matter: An enhanced position layout for efficient context compression in large  
704 language models, 2025. URL <https://arxiv.org/abs/2409.14364>.  
705  
706  
707  
708  
709  
710  
711  
712  
713  
714  
715  
716  
717  
718  
719  
720  
721  
722  
723  
724  
725  
726  
727  
728  
729  
730  
731  
732  
733  
734  
735  
736  
737  
738  
739  
740  
741  
742  
743  
744  
745  
746  
747  
748  
749  
750  
751  
752  
753  
754  
755

756 

## A EXPERIMENT DETAILS

759 We perform pretraining and finetuning using bf16 precision on 8 NVIDIA RTX 3090 GPUs (24GB).  
 760 For pretraining, we randomly sample data from the SlimPajama-6B dataset with a token length  
 761 ranging from 510 to 2040. This data is then split into two halves: one for the auto-encoding (AE)  
 762 task and the other for the language modeling (LM) task (the AE half is discarded for models without  
 763 the AE objective). For downstream tasks, we process the MRQA dataset into a (Context, Question,  
 764 Answer) format for finetuning. Detailed hyperparameters can be found in Table 6.

765 

Table 6: Hyperparameters for training

768 Hyperparameter	769 Value
769 Optimizer	770 AdamW
770 Betas	771 (0.9, 0.95)
771 Weight decay	772 0.1
772 Learning rate	773 1e-4 (pretrain) 5e-5 (finetuning)
773 Scheduler	774 Constant
774 Batch size	775 16
775 Warmup	776 300
776 Training steps	777 20k (pretrain) 20k (finetuning)
777 Clip norm	778 2.0

781 

## B DETAILED RESULTS

782 

### B.1 PRETRAINING RESULTS

786 As shown in Table 7, our method, SAC, achieves the lowest perplexity (10.79) among all baseline  
 787 models. This suggests that removing the autoencoding (AE) objective in SAC allows the model to  
 788 better focus on the language modeling task, thereby improving its predictive capability. Furthermore,  
 789 since SAC avoids the additional computational overhead from independent compression tokens and  
 790 the AE task, its training is approximately 31% faster than ICAE and 26% faster than 500xCompressor  
 791 and EPL.

793 

Table 7: Pretraining comparison of SAC and existing context compression methods, results on LM  
 794 perplexity and training time.

796 Methods	797 LM-PPL	798 Training Time(h)
798 ICAE	12.35	3.85
799 500xCompress	11.83	3.60
800 EPL	10.88	3.60
801 SAC	<b>10.79</b>	<b>2.66</b>

802 

### B.2 ABLATION RESULTS

806 In the main text, we have discussed the significant performance gains of SAC over all baseline  
 807 methods. To provide more detailed evidence, we present the full ablation study results here. As  
 808 shown in Table 8 and Table 9, our conclusion holds not only in terms of average performance but is  
 809 also consistently validated on each individual dataset.

810  
811 Table 8: Ablation studies for SAC under a 5x compression rate on the in-domain dataset are conducted  
812 in three sets: component ablation, token selection, and the influence of the auto-encoding (AE) task.  
813

Methods	SQuAD		NewsQA		TriviaQA		SearchQA		HotpotQA		NQ		Avg	
	F1	EM	F1	EM	F1	EM	F1	EM	F1	EM	F1	EM	F1	EM
<i>Component Ablation</i>														
SAC	65.37	44.83	49.39	27.14	65.06	55.93	69.99	58.06	67.41	50.28	64.56	45.44	63.63	46.95
SAC(w/o mask)	60.21	39.93	45.93	25.74	62.60	53.27	66.66	54.82	64.63	47.43	61.53	42.55	60.26	43.96
SAC(w/o anchor)	61.69	41.72	46.52	25.45	63.90	54.81	68.03	56.17	65.25	48.31	62.21	43.88	61.27	45.06
<i>Token Selection</i>														
SAC(Random)	52.27	33.41	39.51	19.90	59.24	50.22	68.06	55.87	58.84	41.86	56.57	37.86	55.75	39.85
SAC(Lingua-2)	64.89	44.28	48.92	27.11	64.55	55.13	69.89	58.04	67.05	49.74	64.23	44.93	63.26	46.54
<i>AE Effect</i>														
500x(w/ LM only)	44.71	28.89	37.24	20.39	58.97	50.19	65.67	53.74	56.74	40.52	56.07	38.45	53.23	38.70
500x(w/ AE+LM)	51.62	33.63	39.70	22.63	57.62	48.76	66.43	54.38	59.10	42.20	57.11	39.26	55.26	40.14
SAC(w/ AE only)	56.98	37.60	41.09	20.61	58.19	49.08	64.02	51.65	61.58	44.13	57.23	38.98	56.55	40.34
SAC(w/ AE+LM)	64.68	44.62	46.64	25.62	63.34	54.27	68.40	56.48	66.61	49.72	62.56	44.06	62.04	45.80

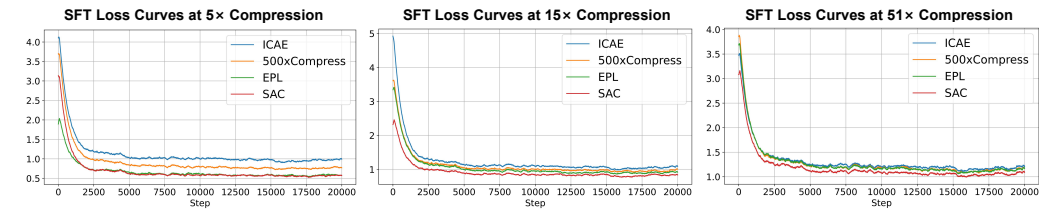
825  
826 Table 9: Ablation studies for SAC under a 5x compression rate on the out-of-domain dataset are  
827 conducted in three sets: component ablation, token selection, and the influence of the auto-encoding  
828 (AE) task.  
829

Methods	BioASQ		DROP		DuoRC		RACE		RE		TQA		Avg	
	F1	EM	F1	EM	F1	EM	F1	EM	F1	EM	F1	EM	F1	EM
<i>Component Ablation</i>														
SAC	44.66	31.45	41.55	30.87	39.48	26.92	30.53	6.23	77.87	65.40	52.24	32.93	47.72	32.30
SAC(w/o mask)	41.93	30.65	40.24	28.48	36.48	23.58	28.21	5.49	69.09	55.63	48.29	29.67	44.04	28.92
SAC(w/o anchor)	43.70	31.78	40.55	30.34	36.97	25.58	30.05	6.82	75.88	62.35	51.59	32.20	46.46	31.51
<i>Token Selection</i>														
SAC(Random)	43.18	30.59	37.67	27.21	23.44	14.59	22.48	5.64	66.79	51.39	45.36	29.27	39.82	26.45
SAC(Lingua-2)	44.49	31.91	41.50	29.61	39.47	26.58	29.96	7.12	77.67	65.47	51.46	32.07	47.43	32.13
<i>AE Effect</i>														
500x(w/ LM only)	43.54	33.11	35.40	25.82	27.71	17.59	19.73	3.86	62.31	48.27	40.60	25.75	38.22	25.73
500x(w/ AE+LM)	40.30	28.99	35.40	25.55	29.43	19.32	21.57	4.90	65.43	50.88	38.62	22.75	38.46	25.40
SAC(w/ AE only)	40.85	29.39	35.32	25.28	31.55	21.32	25.86	4.90	72.29	57.90	46.61	29.08	42.08	27.98
SAC(w/ AE+LM)	44.84	32.31	41.47	31.14	39.29	27.58	30.11	6.23	77.12	64.42	50.74	31.87	47.26	32.26

## C VISUALIZATION ANALYSIS

### C.1 TRAINING CURVES ANALYSIS

847 Figure 6 shows the training loss curves at different compression ratios on the MRQA dataset. The  
848 training loss of our SAC model consistently converges better than other baseline methods across  
849 all compression ratios, which demonstrates that the compressed representations obtained from the  
850 SAC architecture are more beneficial for language modeling tasks. Notably, as the compression ratio  
851 increases appropriately, the difference in convergence between SAC and the other baselines becomes  
852 more significant.



862 Figure 6: Supervised finetuning loss curves. The figure illustrates the training loss trajectories of  
863 different models under three compression ratios: 5x, 15x, and 51x.

864  
865

## C.2 ATTENTION ANALYSIS

866  
867  
868  
869  
870  
871  
872

At a lower 5x compression rate, as shown in Figure 7, the attention map of EPL presents a clear positive diagonal, indicating that its compressed tokens primarily attend to local tokens. In contrast, the attention map of 500xCompressor appears more diffused, while our SAC model exhibits a sparse and highly focused attention pattern, with its anchor tokens attending to only a few key original context tokens. This phenomenon becomes more pronounced with increasing compression rates, being most evident at the 51x compression rate in Figure 9, which strongly demonstrates the robustness of SAC in extreme compression environments.

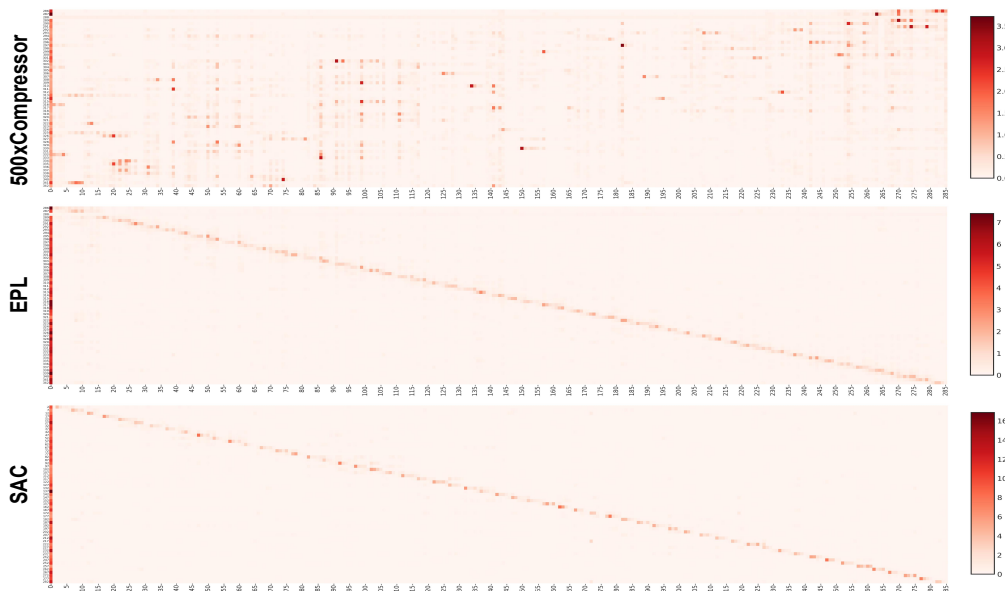
873  
874  
875  
876  
877  
878  
879  
880  
881  
882  
883  
884  
885  
886  
887  
888  
889  
890  
891  
892893  
894  
895  
896

Figure 7: Attention maps of different models finetuned under a 5x compression rate. From top to bottom, the figure displays the final layer attention maps for the 500xCompressor, EPL, and SAC models, respectively. The x-axis represents the original context tokens, and the y-axis represents the compression tokens.

897

898

899

## D THE USE OF LARGE LANGUAGE MODELS

900  
901  
902  
903  
904  
905  
906

We used a large language model (LLM) as a general-purpose assist tool. The LLM’s primary role was in assisting with writing and text editing, such as refining prose and correcting grammar and spelling to ensure the paper’s professionalism and fluency. We explicitly state that the LLM was not involved in the core ideation or methodological design of this research. All core contributions of the paper, including the proposal of the methodology, the construction and execution of experiments, and the analysis of results, were performed independently by the authors.

907  
908  
909  
910  
911  
912  
913  
914  
915  
916  
917

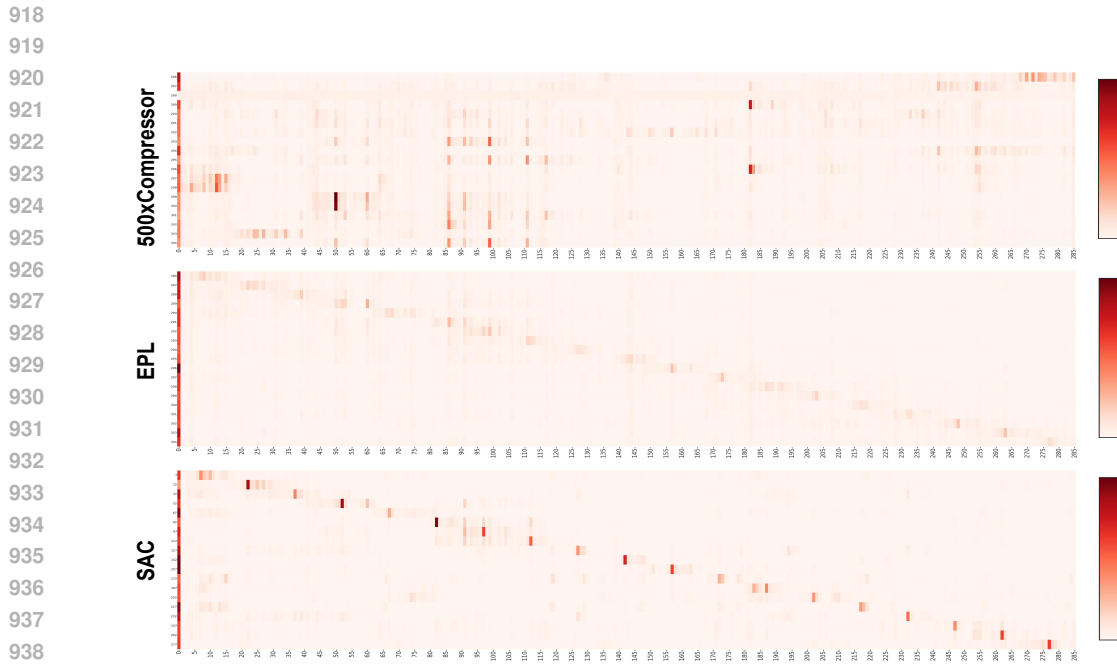


Figure 8: Attention maps of different models finetuned under a 15x compression rate. From top to bottom, the figure displays the final layer attention maps for the 500xCompressor, EPL, and SAC models, respectively. The x-axis represents the original context tokens, and the y-axis represents the compression/anchor tokens.

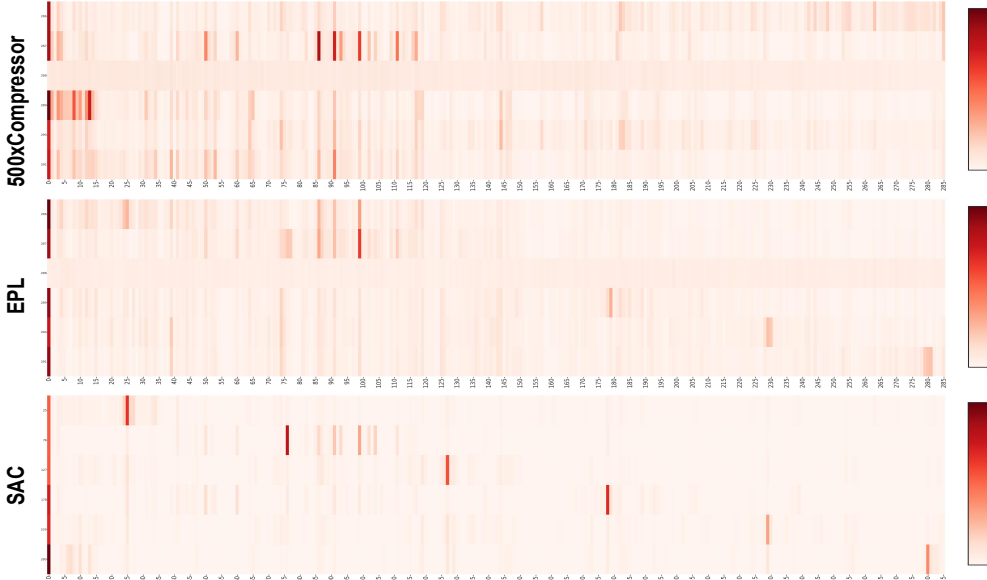


Figure 9: Attention maps of different models finetuned under a 51x compression rate. From top to bottom, the figure displays the final layer attention maps for the 500xCompressor, EPL, and SAC models, respectively. The x-axis represents the original context tokens, and the y-axis represents the compression tokens.

972  
973  
974  
975  
976  
977  
978  
979  
980  
981  
982  
983  
984  
985  
986  
987  
988  
989  
990  
991  
992  
993  
994  
995  
996  
997  
998  
999  
1000  
1001  
1002  
1003  
1004  
1005  
1006  
1007  
1008  
1009  
1010  
1011  
1012  
1013  
1014  
1015  
1016  
1017  
1018  
1019  
1020  
1021  
1022  
1023  
1024  
1025

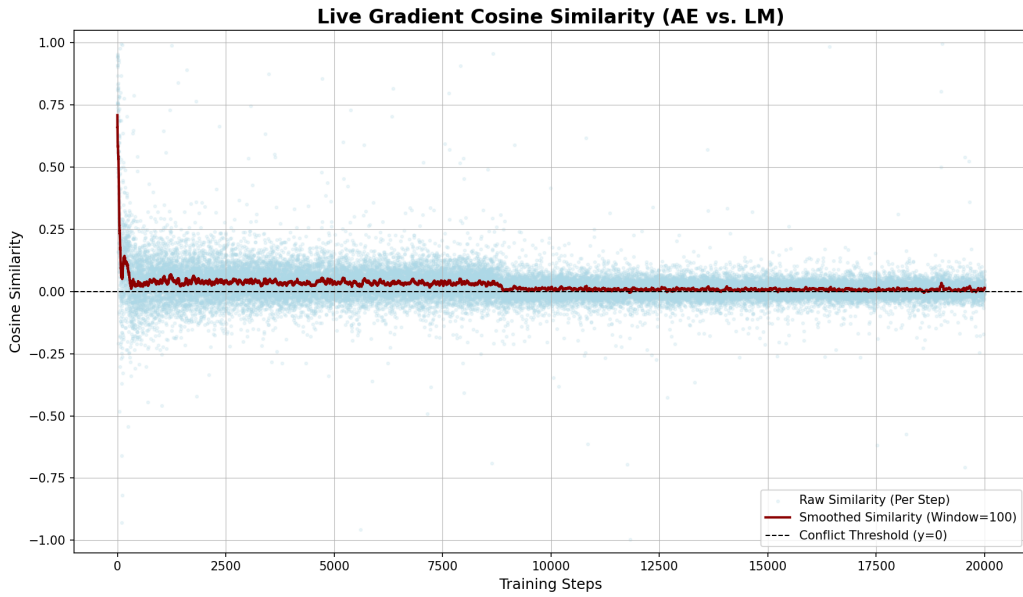


Figure 10: Gradient Cosine Similarity between AutoEncoder (AE) Loss and Language Modeling (LM) Loss.

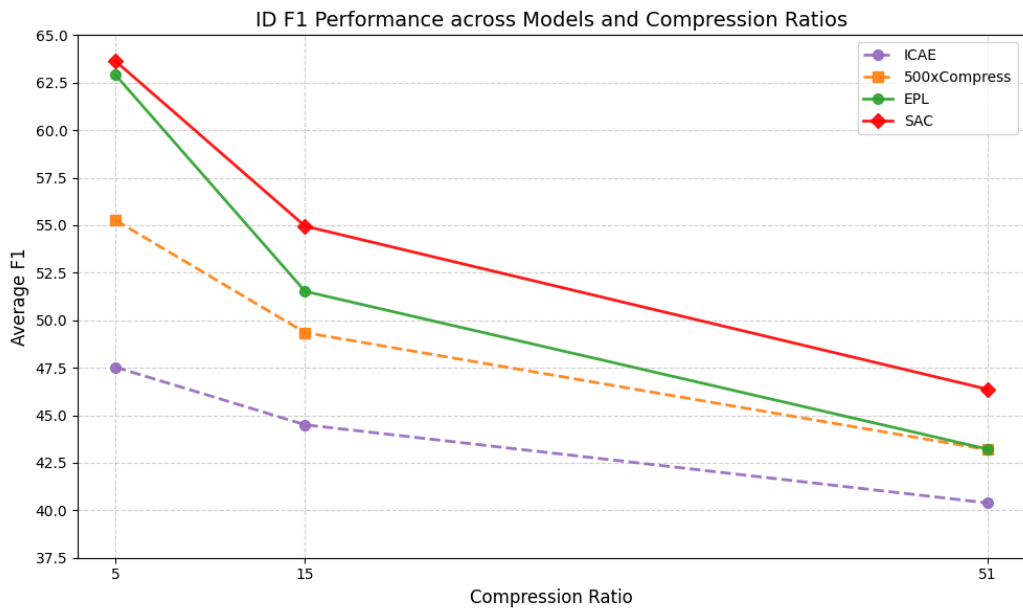


Figure 11: Efficiency and Performance Trade-off Curves on In-Domain (ID) Tasks.